Analytical investigation of higher-order plasmonic modes on a metal-dielectric interface

Mahdi Kordi, Fahimeh Armin, Mohammad R. Malekfar, Mir Mojtaba Mirsalehi, and Mehrdad Shokooh-Saremi
Department of Electrical Engineering, Faculty of Engineering, Ferdowsi University of Mashhad, Mashhad 9177948974, Iran
(Received 15 November 2016; published 20 March 2017)

Based on the plane-wave expansion method, we have analytically obtained a set of higher-order transverse magnetic (TM) modes that can exist on a metal-dielectric interface. Any linear combination of these modes can be supported on the interface. Our analysis is based on the assumption of nonuniformity of the electromagnetic fields in all directions. We have also shown that no higher-order transverse electric (TE) mode can propagate on the interface. Furthermore, the orientation of Poynting vector and energy flow of the TM modes are described. Our results show that the Poynting vector of a higher-order TM mode always makes an angle with the interface, which means TM modes are not pure surface waves.

DOI: 10.1103/PhysRevA.95.033824

I. INTRODUCTION

In the recent decades, extensive studies have been carried out on investigation and analysis of surface waves, since they would make it possible to transfer information on a planar waveguide. Among different kinds of surface waves, surface plasmon polaritons have attracted more interest because of their ability in transmitting energy below the diffraction limit of light [1–3].

Despite several valuable theoretical and experimental research on surface plasmon waves, few of them have considered higher-order plasmonic modes. Although single mode description of plasmonic waves results in acceptable outcomes in many applications, there exist some cases that cannot be explained by this description [4,5]. Higher-order plasmonic modes have been studied, both theoretically and experimentally, in nanowires and ribbon waveguides with finite widths [6–9]. The work done by Zakharian *et al.* is one of the first investigations on higher-order modes in metallic slab waveguide structures [10]. Based on the study presented by Zakharian *et al.* and referring to their earlier analytical work, Norrman *et al.* studied higher-order modes supported by a metal film sandwiched between two similar dielectrics, and showed that an infinite number of modes can be supported by a metallic slab waveguide [11,12]. In both of these works, a two-dimensional structure has been studied. Martinez-Herrero *et al.* have also studied higher-order modes but in the concept of plasmon packet where a Gaussian function has been used to describe the packet and then calculate its propagation length and polarization properties [13]. Another interesting point about surface plasmons has been provided in the analytical work of Gawhary *et al.* [14]. Considering the single mode description, they have shown that a surface plasmon mode propagating on a metal-dielectric interface is neither a TE nor a TM pure surface wave.

In contrast to previous works, we have focused on nonuniform electromagnetic fields of a metal-dielectric interface. Based on the plane-wave expansion method, we have obtained a set of higher-order orthogonal transverse magnetic (TM) modes for this interface. All of these modes satisfy Maxwell's equations and the electromagnetic boundary conditions. Hence any linear combination of these modes can be supported on the interface. We also show that, in addition to the fundamental mode [14], higher-order TM modes are not pure surface waves. For better understanding theses higher-order modes, we have also shown how their energy flows differ from the corresponding flow of the fundamental mode.

The structure of this paper is as follows. We start with a brief review of the solution to the Helmholtz wave equation for a two-dimensional structure. Then, the TM and transverse electric (TE) modes are studied. Next, the hybrid modes are investigated, in which none of the fields components are zero. The Poynting vector and energy flow of the TM modes are discussed in the next section. The last section is devoted to Conclusion.

II. BACKGROUND

The simplest structure capable of carrying a surface plasmon wave consists of two semi-infinite regions of a dielectric and a metal as shown in Fig. 1.

In this figure, z axis is the wave propagation direction and x axis is normal to the surface. It is usually assumed that the plasmonic wave is uniform in the y direction, i.e., $\partial/\partial y = 0$ [15–17]. Solving the Helmholtz wave equation based on this assumption shows that TE surface modes cannot exist, but a TM mode having a propagation constant of

$$\beta = k_0\sqrt{\frac{\varepsilon_1\varepsilon_2}{\varepsilon_1+\varepsilon_2}} \tag{1}$$

is supported, where ε_1 and ε_2 are the dielectric constants of the two media and k_0 is the wave number in free space. We consider this mode as the fundamental mode of the structure (TM_0). The assumption $\partial/\partial y = 0$ would not reveal any higher-order modes.

In the following sections, we investigate the solutions of the wave equation without using the uniformity assumption in the y direction. First, we start with TM and TE modes of higher orders and then move on to investigate the possibility of existence of hybrid modes.

III. TM_x MODES

In Fig. 1, the discontinuity of the structure is in the x direction. Therefore, we expect the structure to support higher-order magnetic modes which are transverse to the x direction (TM_x). Note that in the case of TM_0 mode, the

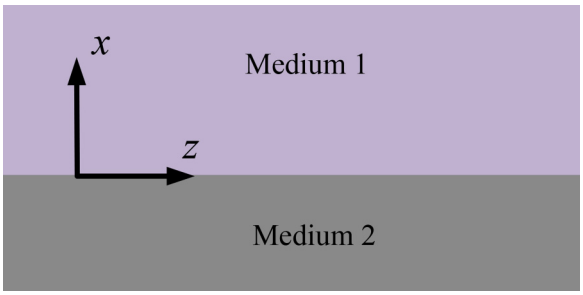

FIG. 1. Schematic of a metal-dielectric interface.

components of magnetic field in x and z directions are both zero and therefore this mode can be considered TM_x or TM_z.

Starting with the magnetic vector potential $\boldsymbol{A}$, for the two media as

$$\boldsymbol{A_1} = A_1 e^{-k_{x1}x} e^{-k_y y} e^{-j\beta z} \boldsymbol{a_x}, \quad x \geqslant 0, \tag{2}$$

$$\boldsymbol{A_2} = A_2 e^{k_{x2}x} e^{-k_y y} e^{-j\beta z} \boldsymbol{a_x}, \quad x < 0, \tag{3}$$

and following the trend presented in classical electromagnetic references [18,19], one can obtain the magnetic fields in the two media as

$$\boldsymbol{H_1} = \frac{\nabla \times \boldsymbol{A_1}}{\mu_0} = \left(-j\beta \frac{A_1}{\mu_0} \boldsymbol{a_y} + k_y \frac{A_1}{\mu_0} \boldsymbol{a_z}\right) \times e^{-k_{x1}x} e^{-k_y y} e^{-j\beta z}, \tag{4}$$

$$\boldsymbol{H_2} = \frac{\nabla \times \boldsymbol{A_2}}{\mu_0} = \left(-j\beta \frac{A_2}{\mu_0} \boldsymbol{a_y} + k_y \frac{A_2}{\mu_0} \boldsymbol{a_z}\right) \times e^{k_{x2}x} e^{-k_y y} e^{-j\beta z}. \tag{5}$$

In the above equations, $\nabla\times$ represents the curl operation, μ_0 is the permeability of vacuum, A_1 and A_2 are magnitudes of the magnetic vector potentials in the two media, and k_{x1} and k_{x2} are the x components of the corresponding wave vectors. Also, k_y is the y component of the wave vector in the two media and β is the propagation constant in z direction. The boundary condition for the tangential magnetic fields at the yz plane results in the equality of amplitudes, i.e., $A_1 = A_2$.

The electric fields can be obtained using Maxwell's equations

$$\boldsymbol{E_1} = \frac{1}{j\omega\mu_0\varepsilon_0\varepsilon_1}\left((\beta^2 - k_y^2)\boldsymbol{a_x} + k_{x1}k_y\boldsymbol{a_y} + jk_{x1}\beta\boldsymbol{a_z}\right) \times A_1 e^{-k_{x1}x} e^{-k_y y} e^{-j\beta z}, \tag{6}$$

$$\boldsymbol{E_2} = \frac{1}{j\omega\mu_0\varepsilon_0\varepsilon_2}\left((\beta^2 - k_y^2)\boldsymbol{a_x} - k_{x2}k_y\boldsymbol{a_y} - jk_{x2}\beta\boldsymbol{a_z}\right) \times A_2 e^{k_{x2}x} e^{-k_y y} e^{-j\beta z}. \tag{7}$$

The boundary condition for the tangential components of electric fields results in

$$\frac{k_{x1}}{\varepsilon_1} = -\frac{k_{x2}}{\varepsilon_2}. \tag{8}$$

Also, the following dispersion relations hold for the electromagnetic wave:

$$\varepsilon_1 k_0^2 + k_{x1}^2 + k_y^2 - \beta^2 = 0, \tag{9}$$

$$\varepsilon_2 k_0^2 + k_{x2}^2 + k_y^2 - \beta^2 = 0. \tag{10}$$

For the fundamental mode of the structure, where uniformity in y direction imposes $k_y = 0$, using Eqs. (8)–(10) reveals the propagation constant of the surface plasmon as Eq. (1). However, for higher-order TM_x modes, where $k_y \neq 0$, the propagation constants cannot be calculated from these equations, since there are four unknown parameters and three equations. This degree of freedom reveals infinite number of modes. Subtracting Eq. (10) from Eq. (9) will reveal a relation between k_{x1} and k_{x2} as

$$k_{x1}^2 - k_{x2}^2 = k_0^2(\varepsilon_2 - \varepsilon_1). \tag{11}$$

Using this equation in conjunction with Eq. (8), the following expressions are obtained:

$$k_{x1} = \pm\frac{jk_0\varepsilon_1}{\sqrt{\varepsilon_1 + \varepsilon_2}}, \tag{12}$$

$$k_{x2} = \mp\frac{jk_0\varepsilon_2}{\sqrt{\varepsilon_1 + \varepsilon_2}}. \tag{13}$$

Mathematically both negative and positive signs are valid but, to have a physical mode, the real parts of k_{x1} and k_{x2} should be positive. Therefore, with respect to the $\pm$ sign in Eq. (12), the multiplication of the real parts of k_{x1} and k_{x2} must be positive. So, the relation

$$\mathrm{Re}\left\{\frac{j\varepsilon_1}{\sqrt{\varepsilon_1 + \varepsilon_2}}\right\}\mathrm{Re}\left\{\frac{j\varepsilon_2}{\sqrt{\varepsilon_1 + \varepsilon_2}}\right\} < 0 \tag{14}$$

should be satisfied between ε_1 and ε_2.

Equations (12) and (13) show that all TM_x modes have the same propagation constant in the x direction and therefore the same confinement in this direction. It should be mentioned that writing similar trend used here would not reveal any solution for TM_z or TM_y.

To provide a clear picture, the z component of electric field on the metal-dielectric interface ($x = 0$) is shown in Fig. 2 for the fundamental mode and a higher-order TM mode. The fields are calculated for the interface of silver (medium 2) and vacuum (medium 1) at the wavelength of 633 nm. The dielectric constant of silver is obtained from the Palik database [20]. Figure 2(a) corresponds to the fundamental mode where k_y is zero. As can be seen, the wave is uniform in the y direction and propagates in the z direction. Figure 2(b) corresponds to a higher-order TM mode with $k_y = j0.01k_0$. As a result of nonuniformity in the y direction, the propagation direction is deviated from the z axis.

IV. TE_x MODES

It is shown that the zero-order TE mode (TE_0) is not supported by a metal-dielectric interface [16]. To fulfill this discussion over all transverse electric modes, higher-order TE modes will be studied. Using the same procedure as TM modes, one can obtain the electric and magnetic fields for TE_x

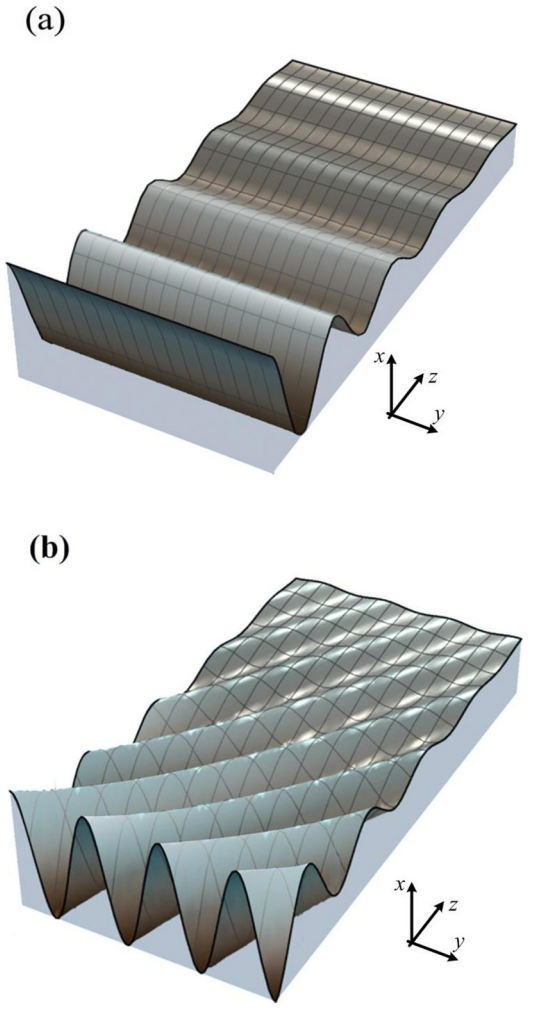

FIG. 2. z component of electric field corresponding to (a) the fundamental mode and (b) a higher-order TM mode on the silver-vacuum interface.

modes from the electric vector potentials. The resulted electric fields for the two media are

$$\boldsymbol{E_1} = \frac{-\nabla \times \boldsymbol{F_1}}{\varepsilon_0\varepsilon_1} = \left(\frac{j\beta F_1}{\varepsilon_0\varepsilon_1}\boldsymbol{a_y} - \frac{k_y F_1}{\varepsilon_0\varepsilon_1}\boldsymbol{a_z}\right) \times e^{-k_{x1}x}e^{-k_y y}e^{-j\beta z}, \quad x \geqslant 0, \tag{15}$$

$$\boldsymbol{E_2} = \frac{-\nabla \times \boldsymbol{F_2}}{\varepsilon_0\varepsilon_2} = \left(\frac{j\beta F_2}{\varepsilon_0\varepsilon_2}\boldsymbol{a_y} - \frac{k_y F_2}{\varepsilon_0\varepsilon_2}\boldsymbol{a_z}\right) \times e^{k_{x2}x}e^{-k_y y}e^{-j\beta z}, \quad x < 0, \tag{16}$$

where F_1 and F_2 are the magnitudes of the electric vector potentials in the upper and lower media, respectively. Equating the tangential components of the electric fields at the yz plane reveals the condition

$$\frac{F_1}{\varepsilon_1} = \frac{F_2}{\varepsilon_2}. \tag{17}$$

Also, the magnetic fields are obtained as

$$\boldsymbol{H_1} = \frac{1}{j\omega\mu_0\varepsilon_0\varepsilon_1}\left(\left(\beta^2 - k_y^2\right)\boldsymbol{a_x} + k_{x1}k_y\boldsymbol{a_y} + jk_{x1}\beta\boldsymbol{a_z}\right) \times F_1 e^{-k_{x1}x}e^{-k_y y}e^{-j\beta z}, \tag{18}$$

$$\boldsymbol{H_2} = \frac{1}{j\omega\mu_0\varepsilon_0\varepsilon_2}\left(\left(\beta^2 - k_y^2\right)\boldsymbol{a_x} - k_{x2}k_y\boldsymbol{a_y} - jk_{x2}\beta\boldsymbol{a_z}\right) \times F_2 e^{k_{x2}x}e^{-k_y y}e^{-j\beta z}. \tag{19}$$

The boundary condition for the tangential components of magnetic fields gives

$$F_1\frac{k_{x1}}{\varepsilon_1} = -F_2\frac{k_{x2}}{\varepsilon_2}. \tag{20}$$

Combining this equation with Eq. (17) would result in

$$k_{x1} = -k_{x2}. \tag{21}$$

To have a physical mode at the interface of two media, the real parts of both k_{x1} and k_{x2} should be positive. According to Eq. (21), the TE_x modes do not satisfy this condition. Therefore, like TE_0, these modes are not supported by the structure shown in Fig. 1. Similarly, it can be shown that other transverse electric modes (TE_y and TE_z) are not supported.

V. HYBRID MODES

Here, we investigate the possibility of existence of hybrid modes. These modes have the most general form where, unlike the cases in the previous sections, none of the fields components are zero. One can express the fields of a hybrid mode as a summation of TE and TM parts. Each of these two parts satisfy Maxwell's equations but do not necessarily satisfy the boundary conditions. Indeed, their summation should fulfill the electromagnetic boundary conditions [21]. As before, we start with the magnetic and electric vector potentials $\boldsymbol{A}$ and $\boldsymbol{F}$ for the two media as

$$\boldsymbol{A_1} = A_1 e^{-k_{x1}x}e^{-k_y y}e^{-j\beta z}\boldsymbol{a_x}, \quad x \geqslant 0, \tag{22}$$

$$\boldsymbol{F_1} = F_1 e^{-k_{x1}x}e^{-k_y y}e^{-j\beta z}\boldsymbol{a_x}, \quad x \geqslant 0, \tag{23}$$

$$\boldsymbol{A_2} = A_2 e^{k_{x2}x}e^{-k_y y}e^{-j\beta z}\boldsymbol{a_x}, \quad x < 0, \tag{24}$$

$$\boldsymbol{F_2} = F_2 e^{k_{x2}x}e^{-k_y y}e^{-j\beta z}\boldsymbol{a_x}, \quad x < 0. \tag{25}$$

The corresponding electromagnetic fields are obtained as

$$\boldsymbol{H_1} = \frac{\nabla \times \boldsymbol{A_1}}{\mu_0} + \frac{\nabla \times \left(\frac{-\nabla \times \boldsymbol{F_1}}{\varepsilon_0\varepsilon_1}\right)}{-j\omega\mu_0} = \left[\left(\frac{\beta^2 - k_y^2}{j\omega\mu_0\varepsilon_0\varepsilon_1}\right)F_1\boldsymbol{a_x} + \left(-j\beta\frac{A_1}{\mu_0} + \frac{k_{x1}k_y F_1}{j\omega\mu_0\varepsilon_0\varepsilon_1}\right)\boldsymbol{a_y} + \left(k_y\frac{A_1}{\mu_0} + \frac{k_{x1}\beta F_1}{\omega\mu_0\varepsilon_0\varepsilon_1}\right)\boldsymbol{a_z}\right] \times e^{-k_{x1}x}e^{-k_y y}e^{-j\beta z}, \quad x \geqslant 0, \tag{26}$$

$$\boldsymbol{H_2} = \frac{\nabla \times \boldsymbol{A_2}}{\mu_0} + \frac{\nabla \times \left(\frac{-\nabla \times \boldsymbol{F_2}}{\varepsilon_0 \varepsilon_2}\right)}{-j\omega\mu_0}$$
$$= \left[\left(\frac{\beta^2 - k_y^2}{j\omega\mu_0\varepsilon_0\varepsilon_2}\right)F_2\boldsymbol{a_x} + \left(-j\beta\frac{A_2}{\mu_0} - \frac{k_{x2}k_yF_2}{j\omega\mu_0\varepsilon_0\varepsilon_2}\right)\boldsymbol{a_y} + \left(k_y\frac{A_2}{\mu_0} - \frac{k_{x2}\beta F_2}{\omega\mu_0\varepsilon_0\varepsilon_2}\right)\boldsymbol{a_z}\right] \times e^{k_{x2}x}e^{-k_yy}e^{-j\beta z}, \quad x < 0, \tag{27}$$

$$\boldsymbol{E_1} = \frac{\nabla \times \left(\frac{\nabla \times \boldsymbol{A_1}}{\mu}\right)}{j\omega\varepsilon_0\varepsilon_1} - \frac{\nabla \times \boldsymbol{F_1}}{\varepsilon_0\varepsilon_1}$$
$$= \left[\left(\frac{\beta^2 - k_y^2}{j\omega\mu_0\varepsilon_0\varepsilon_1}\right)A_1\boldsymbol{a_x} + \left(\frac{k_{x1}k_yA_1}{j\omega\mu_0\varepsilon_0\varepsilon_1} + j\beta\frac{F_1}{\varepsilon_0\varepsilon_1}\right)\boldsymbol{a_y} + \left(\frac{k_{x1}\beta A_1}{\omega\mu_0\varepsilon_0\varepsilon_1} - k_y\frac{F_1}{\varepsilon_0\varepsilon_1}\right)\boldsymbol{a_z}\right] \times e^{-k_{x1}x}e^{-k_yy}e^{-j\beta z}, \quad x \geqslant 0, \tag{28}$$

$$\boldsymbol{E_2} = \frac{\nabla \times \left(\frac{\nabla \times \boldsymbol{A_2}}{\mu}\right)}{j\omega\varepsilon_0\varepsilon_2} - \frac{\nabla \times \boldsymbol{F_2}}{\varepsilon_0\varepsilon_2}$$
$$= \left[\left(\frac{\beta^2 - k_y^2}{j\omega\mu_0\varepsilon_0\varepsilon_2}\right)A_2\boldsymbol{a_x} + \left(-\frac{k_{x2}k_yA_2}{j\omega\mu_0\varepsilon_0\varepsilon_2} + j\beta\frac{F_2}{\varepsilon_0\varepsilon_2}\right)\boldsymbol{a_y} + \left(-\frac{k_{x2}\beta A_2}{\omega\mu_0\varepsilon_0\varepsilon_2} - k_y\frac{F_2}{\varepsilon_0\varepsilon_2}\right)\boldsymbol{a_z}\right] \times e^{k_{x2}x}e^{-k_yy}e^{-j\beta z}, \quad x < 0. \tag{29}$$

These fields should satisfy the electromagnetic boundary conditions. For nonmagnetic media, the normal components of magnetic fields should be equal at the interface. This results in

$$\frac{F_1}{\varepsilon_1} = \frac{F_2}{\varepsilon_2}. \tag{30}$$

Also, the equality of the normal components of the displacement fields ($D = \varepsilon E$) leads to

$$A_1 = A_2. \tag{31}$$

Using Eqs. (30) and (31), the continuity of tangential components of the electric and magnetic fields results in

$$\frac{k_{x1}F_1}{\varepsilon_1} = -\frac{k_{x2}F_2}{\varepsilon_2}, \tag{32}$$
$$\frac{A_1k_{x1}}{\varepsilon_1} = -\frac{A_2k_{x2}}{\varepsilon_2}. \tag{33}$$

Equations (30)–(33) cannot lead to a physical mode, unless $F_1 = F_2 = 0$. Substituting the condition $F_1 = F_2 = 0$ in Eqs. (26)–(29), these equations lead to TM_x solution presented in Sec. III. Therefore, our derivations based on plane-wave expansion result in no hybrid mode for metal-dielectric interface.

Up to this point, we have shown that apart from the zero-order plasmon mode, TM_0, higher-order TM modes can also be supported on a metal-dielectric interface. We have come up with an orthogonal set of modes, where any linear combination of these modes can be a solution. For example, the z component of electric field in medium 1 can be written as

$$E_{1z} = \int_{k_y''=-\infty}^{+\infty}\int_{k_y'=0}^{+\infty} f(k_y', k_y'')e^{-\left(\frac{\pm jk_0\varepsilon_1}{\sqrt{\varepsilon_1+\varepsilon_2}}\right)x}e^{-k_yy}e^{-j\beta z}dk_y'dk_y'', \tag{34}$$

where $f(k_y', k_y'')$ is the amplitude of the mode corresponding to $k_y = k_y' + jk_y''$ and could be any arbitrary function. Equation (34) represents a linear combination of TM_x modes. Martinez-Herrero *et al.* have introduced the concept of surface plasmon packet to show that a metal-dielectric surface can support more than one mode [13]. Their results are a special case of Eq. (34) in which $f(k_y', k_y'') = \delta(k_y')G(k_y'')$, where G is an arbitrary function and δ is the Kronecker delta function.

According to the results obtained here, both β and k_y determine the energy flow of the mode. In fact, if one divides the wave vector to a normal and a tangential component to the surface, the tangential component of wave vector is important for the propagation. In general, k_x, k_y, and β all have complex values; hence the wave vector is complex. This yields that the normal to a constant-phase plane and the normal to a constant-amplitude plane are not parallel. None of these two vectors represent the propagation direction. One should find the Poynting vector to obtain the direction of energy flow.

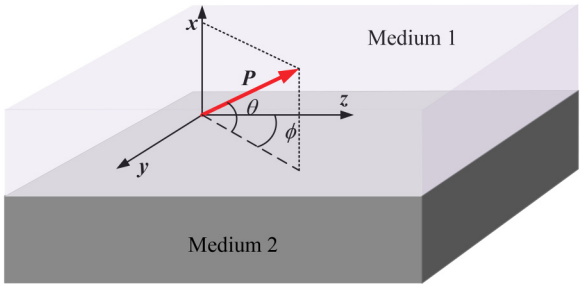

FIG. 3. Poynting vector and the related angles. The dashed line shows the trajectory of $\boldsymbol{P}$ on the yz plane.

VI. POYNTING VECTOR AND ENERGY FLOW

Although all the investigated TM modes in this paper have similar mathematical formulation, they differ in their energy flow directions. The orientation of Poynting vector is schematically shown in Fig. 3. As θ, the angle of Poynting vector ($\boldsymbol{P}$) to the surface, increases, the wave behaves more like a radiation mode, transmitting the energy away from the surface. On the other hand, modes having smaller values of θ are more bounded to the surface. In general, the energy flow direction of a TM_x mode is not in the xz plane and the trajectory of its Poynting vector on the yz plane makes an angle with the z axis (ϕ). TM_0 mode, on the other hand, is uniform in the y direction and therefore its Poynting vector has no y component, i.e., $\phi = 0$. In this section, we study the energy flow of TM_x modes by calculating the angles θ and ϕ for different possible values of k_y.

The Poynting vector $\boldsymbol{P}$ is generally obtained by

$$\boldsymbol{P} = \tfrac{1}{2}\mathrm{Re}(\boldsymbol{E} \times \boldsymbol{H}^*) = P_x\boldsymbol{a_x} + P_y\boldsymbol{a_y} + P_z\boldsymbol{a_z}. \tag{35}$$

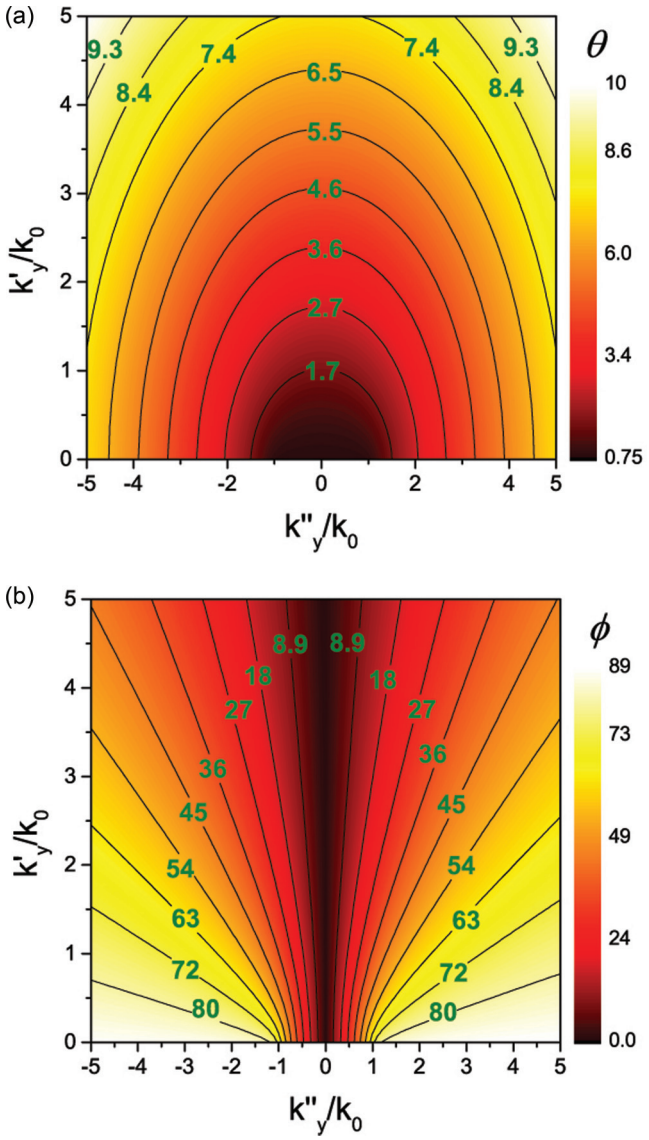

FIG. 4. Values of the angles (a) θ and (b) ϕ corresponding to the Poynting vectors of TM_x modes. These values correspond to medium 1. The values are given in degrees.

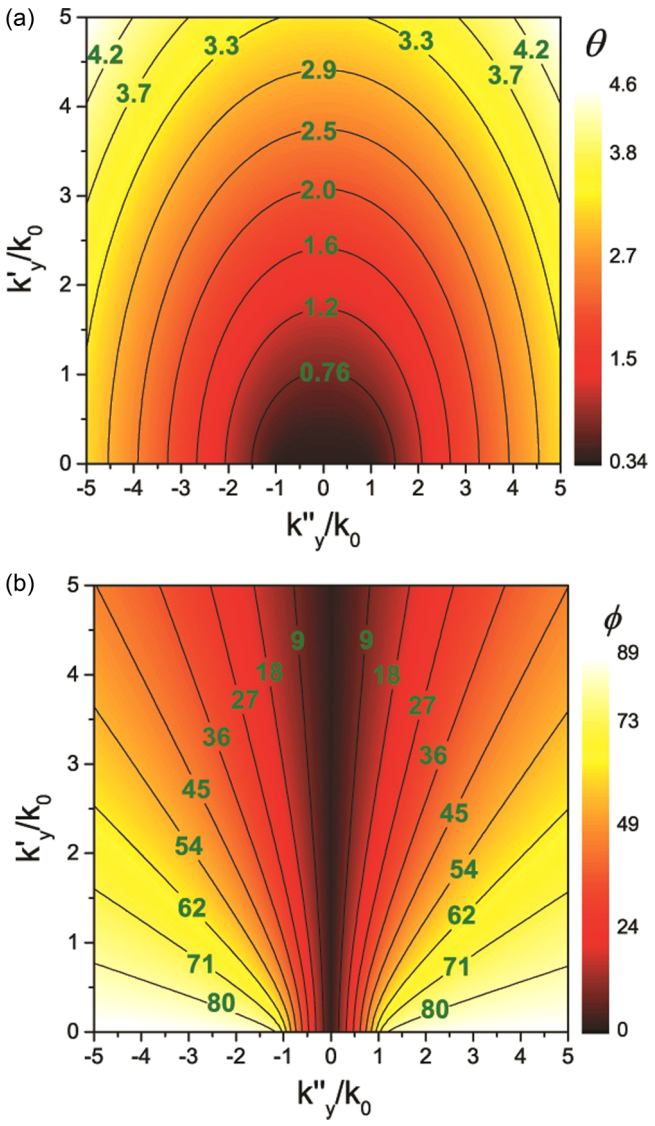

FIG. 5. Values of the angles (a) θ and (b) ϕ corresponding to the Poynting vectors of TM_x modes. These values are calculated in medium 2. The values are given in degrees.

By substituting $\boldsymbol{E}$ and $\boldsymbol{H}$ from Eqs. (4)–(7) in Eq. (35), θ and ϕ can be calculated from

$$\theta = \sin^{-1}\left(\frac{P_x}{|\boldsymbol{P}|}\right), \tag{36}$$

$$\phi = \cos^{-1}\left(\frac{P_z}{|\boldsymbol{P}|\cos(\theta)}\right). \tag{37}$$

As before, media 1 and 2 are assumed to be vacuum and silver, respectively. All calculations have been done for the wavelength of 633 nm. Calculated values of θ and ϕ for the TM_x modes in medium 1 are shown in Fig. 4. According to the notations used in this paper, the imaginary part of k_y, i.e., k_y'', can have positive or negative values, while its real part, i.e., k_y', corresponds to the loss and should be positive. In Fig. 4(a), as the absolute values of k_y' and k_y'' increase, θ increases too, directing more energy away from the surface to the upper medium. The smallest possible value for θ occurs when both real and imaginary parts of k_y are zero, which corresponds to the TM_0 mode. The angle ϕ has its smallest values for TM_x modes with real values of k_y including TM_0 mode. As the absolute value of k_y'' increases, the Poynting vector deviates more from the xz plane. According to Fig. 4(b), ϕ is an increasing function of k_y'' and a decreasing function of k_y'.

The angles θ and ϕ corresponding to the Poynting vectors of TM_x modes in silver are shown in Fig. 5. In general, the results are similar to the ones obtained for the upper medium. As can be seen in Fig. 5(a), the maximum value of θ in medium 2 is smaller, showing that the modes are more confined in the silver.

The determination of angle θ requires having various components such as k_{x1}, k_{x2}, k_y, and β. On the other hand, according to Eq. (12), k_{x1} is identical for all TM_x modes and therefore the penetration depths and also the propagation

constants of the fields above the interface are similar for all TM_x modes. This limits the range of θ.

Our analytical calculations which are graphically represented in Figs. 4 and 5 show that θ is not equal to zero for TM_x modes and therefore these modes are not pure surface waves.

VII. CONCLUSION

In this paper, we have derived higher-order modes of surface plasmon polariton on a metal-dielectric interface using the exact solution of Helmholtz wave equation. Our solution is based on plane-wave expansion and provides a set of orthogonal modes for the structure. It is shown that in addition to the fundamental mode, TM_0, higher-order transverse magnetic modes, TM_x, can also exist. Furthermore, it is shown that higher-order TE modes cannot exist on the interface. We have also investigated hybrid modes, in which none of the components of the electric and magnetic fields are zero. However, our analysis for hybrid modes only reveals TM_x modes for the metal-dielectric interface.

We have investigated the energy flow of higher-order TM modes by calculating the orientation of the Poynting vector. Using the obtained results, the confinement of modes to the surface and their deviations from the propagation direction are analyzed. Our results show that the angle between the Poynting vector and the interface, θ, has its smallest value for the fundamental mode. Also, because of their deviations from the interface, all TM_x modes are not pure surface waves. As θ increases for higher-order TM modes, the wave behaves more like a radiative wave.

[1] J. A. Polo and A. Lakhtakia, Laser Photon. Rev. **5**, 234 (2011).

[2] A. A. Maradudin, R. F. Wallis, and G. I. Stegeman, Prog. Surf. Sci. **33**, 171 (1990).

[3] D. K. Gramotnev and S. I. Bozhevolnyi, Nat. Photon. **4**, 83 (2010).

[4] J. J. Foley, J. M. McMahon, G. C. Schatz, H. Harutyunyan, G. P. Wiederrecht, and S. K. Gray, ACS Photon. **1**, 739 (2014).

[5] A. Archambault, T. V. Teperik, F. Marquier, and J.-J. Greffet, Phys. Rev. B **79**, 195414 (2009).

[6] A. Paul, D. Solis, Jr., K. Bao, W.-S. Chang, S. Nauert, L. Vidgerman, E. R. Zubarev, P. Nordlander, and S. Link, ACS Nano **6**, 8105 (2012).

[7] W. Walasik, A. Rodriguez, and G. Renversez, Plasmonics **10**, 33 (2015).

[8] M. Schmidt and P. Russell, Opt. Express **16**, 13617 (2008).

[9] H.-Y. Li, S. Ruhle, R. Khedoe, A. Koenderink, and D. Vanmaekelbergh, Nano Lett. **9**, 3515 (2009).

[10] A. R. Zakharian, J. V. Moloney, and M. Mansuripur, Opt. Express **15**, 183 (2007).

[11] A. Norrman, T. Setälä, and A. T. Friberg, Opt. Express **22**, 4628 (2014).

[12] A. Norrman, T. Setälä, and A. T. Friberg, Phys. Rev. A **90**, 053849 (2014).

[13] R. Martinez-Herrero, A. Garcia-Ruiz, and A. Manjavacas, Opt. Express **23**, 28574 (2015).

[14] O. E. Gawhary, A. J. L. Adam, and H. P. Urbach, Phys. Rev. A **89**, 023834 (2014).

[15] J. Homola, *Surface Plasmon Resonance Based Sensors* (Springer, Berlin, 2006).

[16] S. A. Maier, *Plasmonics: Fundamentals and Applications* (Springer, New York, 2007).

[17] H. Raether, *Surface Plasmons on Smooth and Rough Surfaces and on Gratings* (Springer, Berlin, 1988).

[18] C. A. Balanis, *Advanced Engineering Electromagnetics* (Wiley, New York, 1989).

[19] J. A. Stratton, *Electromagnetic Theory* (McGraw-Hill Book Company, Inc., New York, 1941).

[20] E. D. Palik, *Handbook of Optical Constants of Solids* (Academic Press, Boston, 1998).

[21] R. E. Collin, *Foundations for Microwave Engineering* (McGraw-Hill Book Company, Inc., New York, 2007).